Submitted to Appl. Phys. Lett.

Fast Characterization of Magnetic Impurities in Single-Wall Carbon Nanotubes

Feng Chen,* Yuyi Xue, Viktor G. Hadjiev, and C. W. Chu†

Texas Center for Superconductivity and Advanced Materials,
University of Houston, Houston, Texas 77204-5002

Pasha Nikolaev and Sivaram Arepalli

G.B. Tech/NASA-JSC, Mail Stop ES-1/GBT,
2101 NASA Road One, Houston, TX 77058

(Dated: October 8, 2003)

Abstract

We have demonstrated that the magnetic susceptibility measurement is a non-destructive, fast and accurate method to determine the residual metal catalysts in a few microgram single-wall carbon nanotube (SWCNT) sample. We have studied magnetic impurities in raw and purified SWCNT by magnetic susceptibility measurements, transmission electron microscopy, and thermogravimetry. The data suggest that the saturation magnetic moment and the effective field, which is caused by the interparticle interactions, decreases and increases respectively with the decrease of the particle size. Methods are suggested to overcome the uncertainty associated.

PACS numbers: 73.63.Fg, 75.20.-g, 75.50.Bb, 75.75.+a

Since the discovery of carbon nanotubes,[1] several synthesis routines have been developed. Currently, all bulk synthesis methods of single-wall carbon nanotubes (SWCNT) make use of metal catalysts, which remain as impurities in the resulting nanotube material. Despite considerable efforts in purifying SWCNTs, it is practically impossible to remove metal impurities completely, since some of the metal particles are protected by graphitic shells. Therefore, characterization of the residual metal impurities in the SWCNTs becomes an important issue.

The nano-particles of many metals and alloys, e.g., Co, Ni, Fe and $Cu_{90}Co_{10}$, etc., can be described as superparamagnetic (SP) above the blocking temperature (T_B).[2] The superparamagnetic behavior can be described by a Langevin-like M_A–H curve (M_A is the anhysteretic magnetization), in a scaling form with the reduced magnetization $\frac{M}{M_S}$ and $\zeta = \frac{M_S H}{k_B T}$:

$$\frac{M}{M_S} = \Big(\coth(v\zeta) - \frac{1}{v\zeta} \Big), \tag{1}$$

where M_S is the saturation moment, which is also called spontaneous magnetization; v is the volume per nanoparticle. In most cases, especially well above the blocking temperature, the Langevin law describes the M–H behavior satisfactorily. However, there are deviations from the Langevin law, which are usually explained by anisotropic, long-range interactions between particles.[3,4]

In this article, we characterized amount and size distribution of iron particles by thermogravimetry analysis (TGA) and transmission electron microscopy (TEM) and compared the results to that of magnetic susceptibility measurements. We demonstrated that the magnetic method can detect a few percent of impurities in raw SWCNT specimens with a total weight as small as 7 μg.

The SWCNT samples were produced by high-pressure carbon monoxide (HiPco) technique,[5,6] using Fe as catalyst. One of them was further purified by "soft-baking"[7] (heating in wet air at 250 °C for 1 day, followed by stirring in HCl, careful washing and drying) to reduce iron content.

The iron particle size distributions were obtained from direct measurements of 200–300 particles in TEM. Mean particle size (d) and size distribution width (σ) were determined by fitting TEM data with log-normal distribution[8]. The weight percentage of iron was measured directly in TGA. 2 – 3 mg of SWCNT was heated to 800 °C at 5 °C/min in flowing air. All carbon (SWCNT, amorphous carbon, etc.) and iron oxidize completely, leaving residue of

Fe_2O_3, from which iron content was calculated. Each sample was measured three times in order to calculate mean and standard deviation of iron content.

The magnetic moment (M) was measured using a Quantum Design MPMS (SQUID). The magnetic fields (H) up to 10^4 Oe were applied. The anhysteretic magnetization is given by $M_A(H) = (M_+(H) + M_-(H))/2$, where M_+ and M_- are the magnetization at the H-increase and the H-decrease branches respectively. We also define the remanent magnetization $M_R(H)$ as $(M_+(H)$ - $M_-(H))/2$, thus $M_R(0)$ corresponds to the remanence usually used to characterize permanent magnets.

Three samples were used: unpurified SWCNT with medium (A) and high (B) iron content, and purified SWCNT with very low iron content (C). In Fig. 1 we display the particle size distributions from the TEM micrographs. Iron content (wt.%) in the samples was determined from TGA measurements described above. These results are presented in Table I.

Fig. 2 shows the anhysteretic M_A–H/T curve for the sample A (1.643 mg weight) at T = 10, 60 and 300 K. It is clear that the curves for $T = 60$ and 300 K overlap when plotted against H/T while the curve for $T = 10$ K is shifted to higher H/T. The overlapped curves can be fitted well using Eq. 1. We can conclude that iron particles in this sample are typical superparamagnets with a blocking temperature between 10 and 60 K.

Fig. 3a compares the remanent magnetization M_R and the anhysteretic magnetization M_A for the sample A. For bulk Fe, M_S^{bulk} is about 220 emu/g and M_R^{bulk} is about 100 emu/g,[2] that is, $M_R^{bulk}/M_S^{bulk} \approx 45\%$. The ratio M_R/M_S for the sample A is very small, $\sim 0.5\%$, which also confirms the superparamagnetic behavior of Fe particles. Assuming $M_S = M_S^{bulk}$, we calculated that the sample A contained 15 wt.% Fe particles of average size 3.2 nm (dashed line in Fig. 3 is the fitting to Eq. 1). On the other hand, iron content measured by TGA was 26.5 wt.%. This suggests that M_S of the iron nanoparticles is about 125 emu/g, about half of M_S^{bulk}, which contradicts previous reports on transition metals. For instance, Co nanoparticles have M_S 25% larger than bulk Co[9,10]. This is probably due to the fact that our particle size is considerably smaller than that was reported by others. In order to obtain the particle size value of 2.89 nm (the mean size measured in TEM) from Eq. 1, we need to have $M_S = 319$ emu/g, which is larger than M_S^{bulk}. This suggests that the interaction between nano-particles is strong, which results an effective magnetostatic energy larger than $M_S H$. Thus, we propose to rewrite Eq. 1 into:

$$\frac{M}{M_S} = \Big(\coth(\beta v \zeta) - \frac{1}{\beta v \zeta} \Big), \tag{2}$$

where the effective permeability $\beta \geq 1$ indicates strong ferromagnetic interparticle interactions. For sample A, $M_S = 125$ emu/g and $\beta = 2.55$.

For sample B (0.918 mg weight), M_S is set to 144 emu/g in order for TGA and magnetic measurements. The deduced β is 1.23 in order for the particle size values from TEM (3.32 nm) and magnetic measurements to coincide.

In contrast, purified sample C (46.69 mg weight) showed much larger $M_R = 0.4$ emu per gram of carbon (emu/goc), and much smaller $M_S = 1.6$ emu/goc (Fig. 3b). In iron, single domain particles exist when the size is less than $\sim$ 10 nm,[2] and the particles should be $>$ 5 nm to have $M_R > 0$ (using magnetic anisotropy $K = 450{,}000$ erg/cm^3).[11] Using $M_R^{bulk} =$ 100 emu/g and $M_S = 170$ emu/g (from the measurements of nanoparticles with different mean size in samples A and B), we can estimate that 42% of Fe nanoparticles have diameter greater than 5 nm, in rough agreement with TEM measurements ($d = 3.68$ nm, $\sigma = 0.9$ nm). This shows that aggregation of iron particles occurred during purification.

We have also tried to consider the effect of particle size distribution. Dashed lines in Fig. 3 show the fit of the experimental data with Langevin function utilizing single effective particle size, while the solid lines are Langevin fits utilizing the log-normal distribution of particle diameters obtained from TEM measurements (Fig. 1). It is obvious that the Langevin fits with single particle size slightly underestimate the iron content. The β value obtained from the Langevin fit utilizing log-normal distribution is also larger than the one obtained using a single particle size. This confirms the above conjecture and shows that the magnetic interactions are enhanced with the decrease of the particle sizes.

To demonstrate the sensitivity of the magnetic method in determining iron content, we conducted the test on a part of sample A that weighs only 7 μg. Fig. 4 shows the anhysteretic magnetization for this sample at 60 K and 300 K. Because of the small sample size, the diamagnetic background due to the sample holder is relatively large. At higher fields, this diamagnetic background dominates the signal, making the total magnetic moment negative. However, at lower fields (where curves taken at 60 K and 300 K coincide) the diamagnetic background contribution is relatively small. We have fitted data from that region with Langevin function, and found that Fe content is underestimated only by a factor of 2, and the average particle size is $\sim$ 3.4 nm (compared to 2.89 $\pm$ 0.06 nm from TEM

and $\sim$ 2.9 nm from magnetic measurement on larger sample using $\beta = 2.55$). This comparison demonstrates that diamagnetic background is a major limitation to the accuracy of magnetization measurements of small samples. However, reliable values of iron content and average particle size can still be obtained for samples as small as 50 μg. Careful measurement and subtraction of diamagnetic background can improve the sensitivity by another order of magnitude.

The experimental findings that M_S and β changes with the particle size make simultaneous determination of the mean particle size and iron content somewhat inaccurate by magnetic susceptibility measurement alone. However, the M_S value for iron particles in HiPco does not vary much (Table I). In fact, if we use $M_S = 135$ emu/g (about half of M_S^{bulk}) and $\beta = 1.7$ for all HiPco samples, we can estimate the metal content within an 8% uncertainty and the average particle size within a 12% uncertainty. In addition, by adopting an empirical relationship between β and the particle size, we can get a particle size value that is much more accurate, especially if the iron content is measured independently by TGA. Combined magnetic and TGA measurements allow one to avoid measuring hundreds of particles in TEM, which is rather time-consuming and tedious procedure. In addition, if one only wants to determine the weight percentage of the Fe impurities, it is sufficient to measure just one magnetization value around 1–2 Tesla at room temperature. Thus this method is very fast and we estimate that the iron content determined this way is reliable within 10%.

Note that magnetization measurement has two major limitations. First, one needs to ensure that particles are indeed single-domain and superparamagnetic, that is, their size does not exceed $\sim$ 5 nm in case of iron. This requirement complies with what has been observed for all unpurified HiPco nanotubes, whereas particle aggregation effects are found in purified HiPco nanotubes. The particle size is known to be significantly larger in nanotubes produced by other techniques (for example, it is 10 – 50 nm in nanotubes produced by pulsed laser vaporization (PLV) technique). Second, it is not clear yet how to proceed with catalysts being a mixture of two or more metals.[12] For example, PLV grows nanotubes efficiently in the presence of 1:1 mixture of Co and Ni, and it is not known whether these metals form alloy particles or segregate. Therefore, magnetization measurements can be considered reliable only for HiPco nanotubes.

In conclusion, we have demonstrated that magnetization measurement is a fast, sensitive

and non-destructive way to determine the average size and amount of iron nanoparticles in HiPco nanotubes.[13] We have also found that M_S for the iron nanoparticles with $\sim$ 3 nm mean size in HiPco nanotubes is about half of that of bulk iron. The magnetic interactions are much stronger for the smaller particle sizes (particle size of 2.89 nm has twice of the magnetic interactions than particles of average size 3.32 nm).

The work is supported by NSF Grant No. DMR-9804325, the T. L. L. Temple Foundation, the John J. and Rebecca Moores Endowment, the State of Texas through the Texas Center for Superconductivity at the University of Houston; and at Lawrence Berkeley Laboratory by the U.S. Department of Energy under Contract No. DE-AC03-76SF00098; and NASA Cooperative Agreement No. NCC-1-02038 through TiiMS, and Lockheed Martin contract NAS9-19100.

* Electronic address: fchen@uh.edu

† Also at: Lawrence Berkeley National Laboratory, Hong Kong University of Science and Technology

[1] S. Iijima, Nature **354**, 56 (1991).

[2] R. M. Bozorth, *Ferromagnetism* (IEEE press, Piscataway, N.J., 1993).

[3] M. Respaud, J. Appl. Phys. **86**, 556 (1999).

[4] P. Allia, M. Coisson, P. Tiberto, F. Vinai, M. Knobel, M. A. Novak, and W. C. Nunes, Phys. Rev. B **64**, 144420 (1999).

[5] P. Nikolaev, M. J. Bronikowski, R. K. Bradley, F. Rohmund, D. T. Colbert, K. A. Smith, and R. E. Smalley, Chem. Phys. Lett. **313**, 91 (1999).

[6] M. J. Bronikowski, P. A. Willis, D. T. Colbert, K. A. Smith, and R. E. Smalley, Journal of Vacuum Science & Technology A – Vacuum Surfaces & Films **19**, 1800 (2001).

[7] I. W. Chiang, B. E. Brinson, A. Y. Huang, P. A. Willis, M. J. Brownikowski, J. L. Margrave, R. E. Smalley, and R. H. Hauge, Journal of Physical Chemistry B **105**, 8297 (2001).

[8] J.-M. Bonard, S. Seraphin, J.-E. Wegrowe, J. Jiao, and A. Chatelain, Chem. Phys. Lett. **343**, 251 (2001).

[9] M. Respaud, J. M. Broto, H. Rakoto, and A. R. Fert, Phys. Rev. B **57**, 2925 (1998).

[10] M. L. Billas, A. Chatelain, and W. A. de Heer, Science **265**, 1682 (1994).

[11] D. N. Fischel, H. B. Crawford, D. A. Douglas, and W. C. Eisler, eds., *American Institute of Physics Handbook* (McGraw-Hill, New York, 1972), 3rd ed.

[12] For the example of Fe and Ni, M_S^{bulk} differs by 4 times, we can determine the percentage of the catalyst impurities with high sensitivity, with relative uncertainty of -50% to +100%.

[13] For example, TGA requires at least 3 runs with 2–3 mg specimens, and becomes unreliable for samples with very low iron content due to baseline drift.

TABLE I: Summary of the parameters for the samples studied (d: mean diameter, N: number of particles counted).

Sample	A (raw HiPco)	B (raw HiPco)	C (purified HiPco)
Fe (TGA)	26.46 ± 2.89 %	50.68 ± 2.52 %	1.526 ± 0.33 %
d (TEM)	2.89 ± 0.06 nm	3.32 ± 0.04 nm	3.68 ± 0.05 nm
σ (TEM)	0.83 nm	0.97 nm	0.91 nm
N	268	283	183
M_S	125 emu/g	144 emu/g	170 emu/g
β	2.55	1.23	~ 1

FIGURE CAPTIONS:

FIG 1.: The size distribution of iron particles in all SWCNT samples, measured from TEM micrographs: (a) Sample A (unpurified HiPco nanotubes), (b) Sample B (unpurified HiPco nanotubes with higher Fe content), (c) Sample C (purified HiPco nanotubes).

FIG. 2: Scaling effect of unpurified HiPco SWCNT (A). The curves above the blocking temperature scale into one curve and show Langevin behavior.

FIG. 3: a) M_R (triangles) is much smaller compared to M_A (circles) for unpurified HiPco SWCNT (A); b) M_R is comparable to M_A for purified HiPco SWCNT (C). Filled and open symbols are data obtained at 300 K and 60 K respectively. The dashed line is the Langevin fit with a single particle size, while the solid line is a better fit considering the log-normal particle size distribution.

FIG. 4: M_A for 7 μg of unpurified HiPco SWCNT (A) at 300 K (open circles) and 60 K (solid circles). The line is the Langevin fit in the region where data taken at 60 and 300 K overlaps.

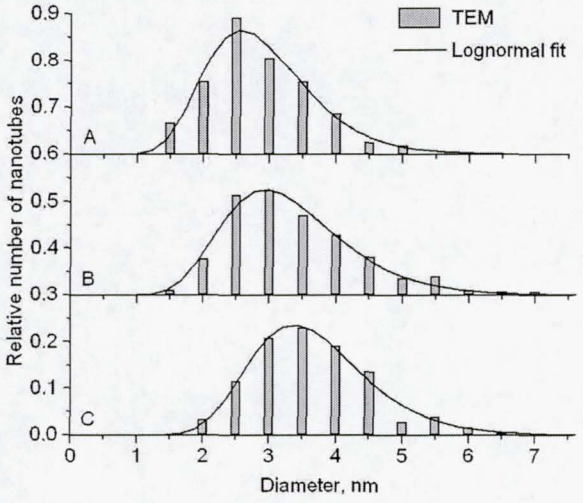

Fig 1

Feng Chen *et al*

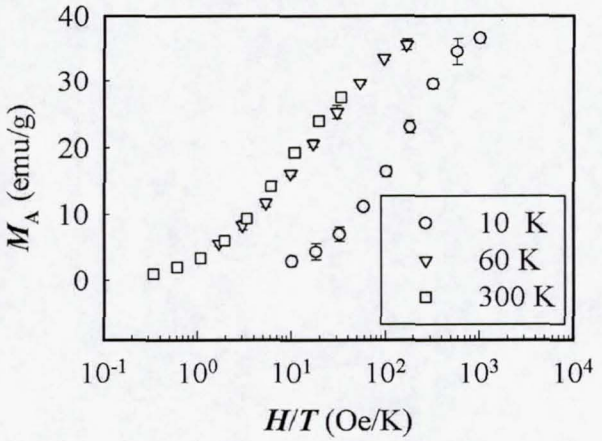

Fig 2

Feng Chen *et al*

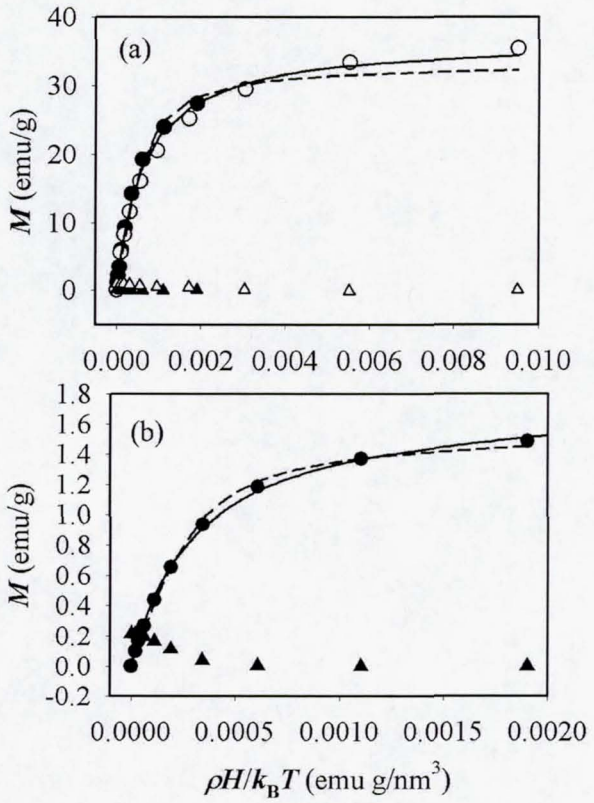

Fig 3

Feng Chen *et al*

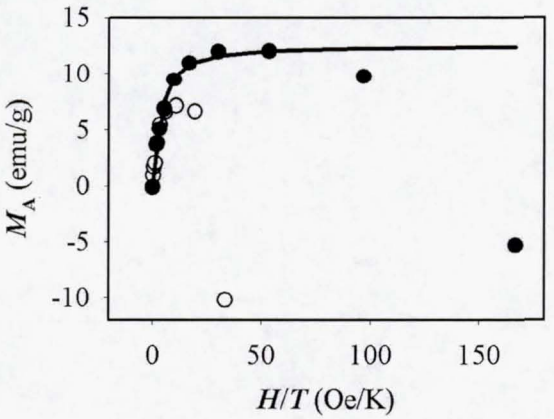

Fig 4

Feng Chen *et al*